



## Development of anode catalysts for a direct ethanol fuel cell

F. VIGIER<sup>1</sup>, C. COUTANCEAU<sup>1</sup>, A. PERRARD<sup>2</sup>, E.M. BELGSIR<sup>1</sup> and C. LAMY<sup>1,\*</sup>

<sup>1</sup>UMR 6503 CNRS – Université de Poitiers, Equipe Electrocatalyse, 40 avenue du Recteur Pineau, 86 022 Poitiers Cedex, France

<sup>2</sup>UPR 5401 (Institut de Recherche sur la Catalyse), Université de Lyon 1, 2 avenue Albert Einstein, 69626 Villeurbanne Cedex, France

(\*author for correspondence, e-mail: [claude.lamy@univ-poitiers.fr](mailto:claude.lamy@univ-poitiers.fr))

Received 6 March 2003; accepted in revised form 11 November 2003

**Key words:** direct ethanol fuel cell, electrooxidation, ethanol, platinum, rhenium, tin

### Abstract

Ethanol electrooxidation was investigated at platinum based electrodes: Pt, Pt–Sn, Pt–Re dispersed on a high surface area carbon powder. The atomic composition of the bimetallic catalyst was varied and the best results were obtained with an atomic ratio Pt:X close to 100:20. The electrocatalytic activity of Pt, PtSn and PtRe was compared using cyclic voltammetry and long-term electrolyses at constant potential. Under voltammetric conditions and in a single direct ethanol fuel cell, PtSn was the most active catalyst. During electrolysis ethanol was oxidized to acetaldehyde (AAL), acetic acid (AA) and carbon dioxide. On PtSn/C and PtRe/C, the ratio AA/AAL was found to be always lower than unity. Otherwise, PtSn electrocatalysts were the most selective towards the production of CO<sub>2</sub> compared to Pt and PtRe electrodes.

### 1. Introduction

The use of fuel cells as clean power sources has been demonstrated and proton exchange membrane fuel cells (PEMFC) have been shown to be one of the most promising devices [1–3]. Different methods of fuel feed are considered: hydrogen from a high-pressure tank [4, 5], hydrogen from methanol or ethanol reforming [6–8], direct methanol [9–11] and direct ethanol fuel cells [12–14]. Because of the drastic decrease in overall mass energy density when hydrogen is stored (Table 1 [15]), the use of a liquid fuel such as alcohol was developed. Alcohols can be either reformed to produce hydrogen which can operate the PEMFC or directly used in the fuel cell. In the first case, the use of a reformer decreases the overall yield of the system and produces a reformat gas containing 1–2% of CO [16, 17] whereas the maximum allowed CO content for a PEMFC is close to 50 ppm [18–20]. This intolerance to fuel impurities requires that a fuel purification processor is put upstream of the anode compartment.

The direct alcohol fuel cell (DAFC) appears to be the most promising system because either methanol in a DMFC or ethanol in a DEFC is not reformed into hydrogen gas but is oxidized directly in the cell. However, DEFCs suffer from difficulties associated with the complete oxidation of ethanol to CO<sub>2</sub>. The catalytic challenge is the breaking of the C–C bond, which is not easily achieved at low temperatures. Although there has

been tremendous progress in the last decade, the most important fundamental research efforts worldwide are currently based on the development of effective anode electrocatalysts.

The high theoretical mass energy density of ethanol makes it a good candidate for PEMFC (Table 1). From the corresponding standard electromotive force  $E_{\text{eq}}^{\circ} = 1.145$  V, the reversible energy efficiency at 25 °C is calculated. Thus,

$$\varepsilon_{\text{rev}} = \frac{nFE_{\text{eq}}^{\circ}}{-\Delta H_{\text{r}}^{\circ}} = \frac{12 \times 96500 \times 1.145}{1366.8 \times 10^3} = 97\% \quad (1)$$

However,  $\varepsilon_{\text{rev}}$  is calculated from thermodynamic data under standard conditions, that is at equilibrium potential with zero current. Under operating conditions, the actual efficiency is given as

$$\varepsilon = \frac{n_{\text{exp}}FE(j)}{-\Delta H_{\text{r}}^{\circ}} = \frac{nFE_{\text{eq}}^{\circ}}{-\Delta H_{\text{r}}^{\circ}} \times \frac{E(j)}{E_{\text{eq}}^{\circ}} \times \frac{n_{\text{exp}}}{n} = \varepsilon_{\text{rev}}\varepsilon_{\text{E}}\varepsilon_{\text{F}} \quad (2)$$

where

$$E(j) = E_2 - E_1 = E_{\text{eq}}^{\circ} - (|\eta_{\text{a}}| + |\eta_{\text{c}}| + |\eta_{\text{Xover}}| + R_{\text{t}}j) \quad (3)$$

$\eta_{\text{a}}$  is the anodic overpotential,  $\eta_{\text{c}}$  the cathodic overpotential,  $\eta_{\text{Xover}}$  the overpotential due to the crossing of

Table 1. Theoretical mass energy density of different fuels

Fuels	Energy densities (/kWh kg <sup>-1</sup> )
H <sub>2</sub>	32.8
H <sub>2</sub> in tank (1.5 wt % storage)	0.42
CH <sub>3</sub> OH	6.1
CH <sub>3</sub> CH <sub>2</sub> OH	8.1
(CH <sub>2</sub> OH) <sub>2</sub>	5.2
NH <sub>3</sub>	5.7
NH <sub>2</sub> -NH <sub>2</sub>	2.6

ethanol through the membrane from the anodic compartment towards the cathodic compartment,  $j$  the current density,  $R_i$  the internal resistance of the cell,  $n_{\text{exp}}$  the experimental number of exchanged electrons and  $n$  the theoretical number of exchanged electrons ( $n=12$  electrons for a complete oxidation of ethanol into CO<sub>2</sub>). As might be expected from Equation 2, the voltage efficiency,  $\varepsilon_E$ , and the faradaic efficiency,  $\varepsilon_F$ , are strongly dependent on electrocatalyst performance: activity at low potentials and selectivity towards CO<sub>2</sub> production for ethanol oxidation and activity at high potentials, selectivity towards H<sub>2</sub>O formation and high tolerance to ethanol for oxygen reduction.

In the present paper, results on the development of anode catalysts for a direct ethanol fuel cell are reported. Particularly, the performance of platinum based electrocatalysts towards ethanol oxidation are compared.

## 2. Experimental details

### 2.1. Electrocatalyst preparation

All electrocatalysts were prepared using the co-impregnation–reduction method [21, 22]. In this method, the carbon support (Vulcan XC 72) was first cleaned at 400 °C for 4 h under pure nitrogen atmosphere, then oxidized in *aqua regia* for 5 min in order to generate functional groups leading to superficial charges. The carbon powder is added to an aqueous solution (ultrapure Water from Millipore MilliQ – 18 MΩ cm) of chloroplatinic acid (H<sub>2</sub>PtCl<sub>6</sub> from Alfa Aesar) either in the presence or in the absence of the metal modifier salts (SnCl<sub>4</sub>, ReCl<sub>3</sub> from Sigma) and stirred for 24 h. The suspension was dried overnight at 70 °C. The resulting powder was then calcined under air for 4 h at 300 °C and reduced under pure hydrogen atmosphere under the same conditions. Pt/C, PtSn/C and PtRe/C electrocatalysts were prepared with a metal loading close to 30% by weight.

### 2.2. Electrode preparation

25 mg of the electrocatalyst powder was added to 0.5 cm<sup>3</sup> of Nafion<sup>®</sup> solution (5 wt % from Aldrich) and 2.5 cm<sup>3</sup> of ultrapure water (Millipore MilliQ – 18 MΩ cm). After ultrasonic homogenisation of the suspension, 2.5 μL were deposited onto a fresh polished

glassy carbon substrate, and the solvent was evaporated under a stream of ultrapure nitrogen at room temperature. A metal loading close to 0.068 mg cm<sup>-2</sup> corresponding to a thickness layer of 1 μm was obtained. The morphology of the dispersed electrocatalyst was examined by transmission electron microscopy (TEM) using a Philips CM 120 microscope.

### 2.3. Electrochemical measurements

The electrochemical equipment consisted of a Wenking potentiostat (model LB75), a waveform generator (Wenking VGS 72) and a XYt recorder (LY1600, Linseis). The electrochemical measurements were carried out in a thermostated three-electrode cell. The supporting electrolyte was 0.1 M HClO<sub>4</sub> (Merk, Suprapure). The counter electrode was a glassy carbon sheet. The reference electrode was a mercury/mercurous sulfate electrode (MSE). The rotation rate of the working electrode was fixed at 3000 rpm for all experiments. All potentials are referred to that of the reversible hydrogen electrode (RHE).

The activity towards ethanol oxidation of dispersed Pt based electrodes with several atomic compositions ranging from 67:33 to pure platinum was evaluated by cyclic voltammetry at a slow sweep rate (5 mV s<sup>-1</sup>) to simulate the steady state conditions. The concentration of ethanol was 0.1 M. and the experiments were carried out at 293 K.

The selectivity of the electrocatalysts was evaluated during long-term electrolyses at 293 K by HPLC (Am-inex Ion Exclusion HPX-87-H column, differential refractometer). Electrolyses were carried out in a two compartment cell separated by a Nafion<sup>®</sup>420 membrane. In the working compartment, the working electrode (4 cm<sup>2</sup>) was prepared as described previously. A glassy carbon was used as counter electrode. Electrolyses were performed for 6 h at a constant potential : 0.35; 0.45; 0.55 and 0.65 V vs RHE.

The operating fuel cell performance was determined in a single DEFC with 5 cm<sup>2</sup> electrodes using a Globe Tech test bench. The  $E=f(j)$  and  $P=f(j)$  curves were recorded using a high power potentiostat (Wenking model HP 88) interfaced with a PC.

Carbon gas diffusion electrodes were homemade using a carbon cloth from Electrochem Inc. painted with the catalytic ink (Metallic catalyst/Vulcan XC72 powder in a PTFE/isopropanol solution). The gas diffusion electrodes were loaded with 4 mg cm<sup>-2</sup> of a mixture of carbon (Vulcan XC/72) and 15 wt% PTFE. Prior to the preparation of the membrane electrode assembly (MEA), the electrodes were heated at 150 °C to recast the Nafion<sup>®</sup> film. The metal loading of the electrodes was close to 1.0 mg cm<sup>-2</sup> and the Nafion<sup>®</sup> loading of the electrode was 0.8 mg cm<sup>-2</sup>. The MEAs were prepared by pressing (35 kg cm<sup>-2</sup> at 130 °C for 90 s) a pretreated Nafion<sup>®</sup>117 membrane with an E-TEK cathode on one side (2.0 mg cm<sup>-2</sup> Pt loading) and the homemade anode on the other side.

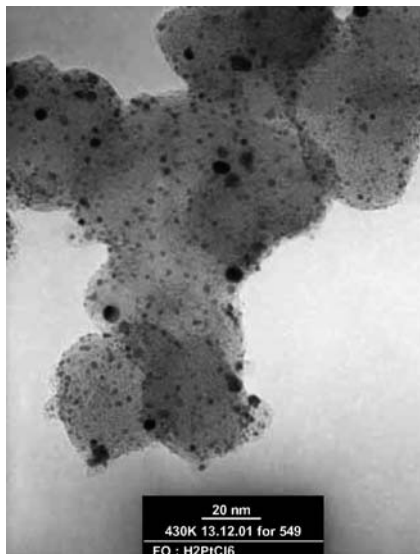


Fig. 1. TEM image recorded at 430 keV of a Pt/C catalyst (30% metal loading) prepared by impregnation–reduction of  $\text{H}_2\text{PtCl}_6$ .

### 3. Results and discussion

#### 3.1. Catalyst characterization

The TEM analysis of a Pt/C electrocatalyst shows that the co-impregnation–reduction method leads to a bimodal particle size distribution centred around 1.5 and 5 nm (Figure 1). The small particles result from electrostatic interactions of the precursor salt with the carbon substrate whereas the large particles are obtained from the reduction of the excess of metal salts. In the absence of electrostatic interactions with the superficial charges of the activated carbon, the metal particles agglomerate during the reduction process. This phenomenon is more drastic when the metal loading is increased.

The EDX spectrum of a PtSn (100:20) electrocatalyst is represented in Figure 2. The atomic ratio calculated

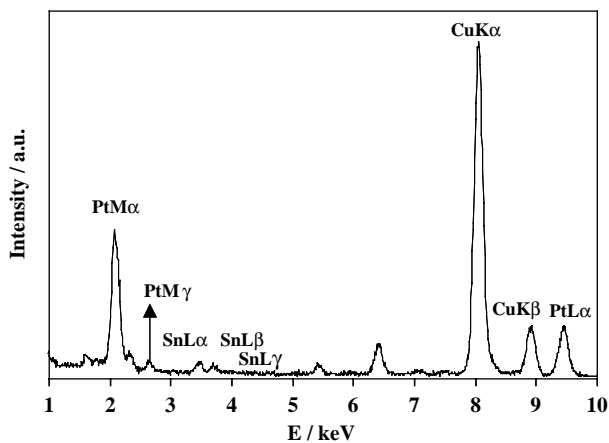
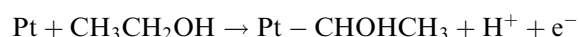
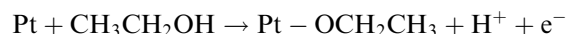


Fig. 2. EDX spectrum of a PtSn (100:20)/C catalyst (30% metal loading) prepared by co-impregnation–reduction of  $\text{H}_2\text{PtCl}_6$  and  $\text{SnCl}_4$ .

using this technique is in excellent agreement with that expected showing that the preparation method by co-impregnation allowed to control easily the atomic composition of the catalysts.

#### 3.2. Cyclic voltammetry

Ethanol oxidation has been extensively studied at platinum electrodes [23–25]. Iwasita and Pastor [24, 25] have shown that ethanol can be O- or C-adsorbed on platinum:



Several mechanisms were proposed to explain the formation of the reaction products at platinum electrodes [23–35]. Depending on the potential, acetaldehyde ( $\text{CH}_3\text{CHO}$ , AAL), acetic acid ( $\text{CH}_3\text{COOH}$ , AA), carbon dioxide ( $\text{CO}_2$ ) and methane ( $\text{CH}_4$ ) are observed. The main products are AAL and AA, which is considered as a final product because it is not oxidized under smooth conditions. The challenge is to avoid the formation of AA by promoting the C–C breaking route from the early adsorption steps. In order to increase the electrocatalyst activity towards ethanol oxidation, platinum was often modified with other metals like Ru [27, 28], Pb [29] or Sn [30, 31]. Delime et al. [30] and Rezzouk et al. [32] have shown that the addition of Sn increases the activity of platinum towards ethanol oxidation.

The effect of the atomic ratio of Pt:Sn catalysts is represented in Figure 3. The onset of the oxidation wave shifted from 0.3 V vs RHE on Pt to 0.1 V vs RHE on Pt–Sn. In the potential range suitable for practical applications in a DEFC ( $0.1 < E < 0.5$  V), Pt:Sn with an atomic composition of 100:20 seems to be the most

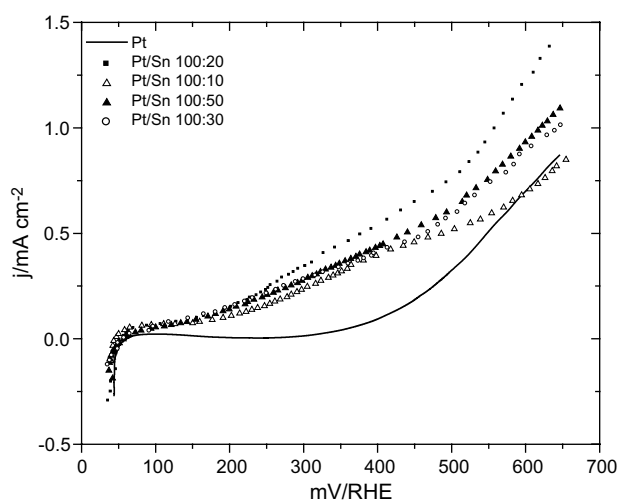


Fig. 3.  $j(E)$  polarization curves for ethanol oxidation on Pt/C and PtSn/C catalysts (30% metal loading). Pt/Sn atomic ratio ranges from 100:10 to 100:50 (0.1 M  $\text{HClO}_4$ , 1.0 M EtOH,  $\nu = 5 \text{ mV s}^{-1}$ ,  $T = 293 \text{ K}$ ).

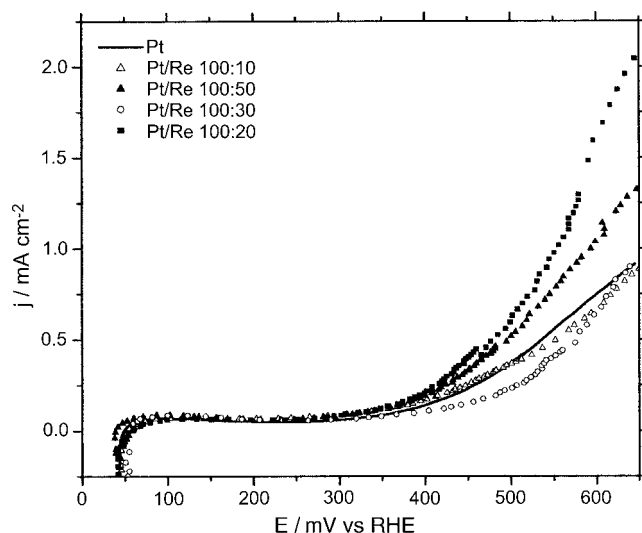


Fig. 4.  $j(E)$  polarization curves for ethanol oxidation on Pt/C and PtRe/C catalysts (30% metal loading). Pt/Re atomic ratio ranges from 100:10 to 100:50 (0.1 M HClO<sub>4</sub>, 1.0 M EtOH,  $\nu = 5 \text{ mV s}^{-1}$ ,  $T = 293 \text{ K}$ ).

active catalyst leading to a relatively good current density,  $0.5 \text{ mA cm}^{-2}$  at  $0.3 \text{ V}$  vs RHE. According to Roman-Martinez et al. [22], the atomic ratio of Pt:Sn plays an important role in the distribution of PtSn and Pt<sub>3</sub>Sn phases in the metal clusters. It seems that an atomic composition close to 100:20 leads to an optimal mixture of the two phases for the ethanol oxidation reaction.

The atomic ratio 100:20 was found to be optimum even in the case of other add-metals like Re. In heterogeneous catalysis rhenium is known to be a good catalyst for the breaking of the C–C bond [33, 34]. PtRe electrocatalysts were also prepared and their electrocatalytic activity is reported in Figure 4. It is only beyond  $0.35 \text{ V}$  that the positive effect of Re is clearly observed. The improvement expected at low potential is not obtained.

### 3.3. Electrolyses

The activity of Pt, PtSn and PtRe electrocatalysts was also evaluated during long term electrolyses carried out at room temperature. At a constant potential the quantity of electricity involved during electrolyses is related to the activity of the electrocatalyst. The positive effect of Sn and Re is clearly shown in Table 2. Whatever the potential PtRe electrocatalysts were the most active. Compared to pure platinum, the positive effect of Sn and Re was decreasing when the electrolysis potential was increased. In fact, pure platinum is known to be active towards ethanol oxidation from  $0.4 \text{ V}$  vs RHE and the gap in current density between Pt on one side and PtSn and PtRe on the other side decreases. The faradaic yield,  $R_F$ , calculated as the ratio between the theoretical quantity of electricity, deduced from the analytical results, and the experimental quantity of

Table 2. Electrolyses of 0.1 M ethanol in perchloric acid medium at  $T = 293 \text{ K}$ . Effect of the nature of the electrocatalysts and of the electrolysis potential on the quantities of electricity and the faradaic yields

Electrolysis potential /V vs RHE	Electrocatalysts	$Q_{\text{EX}}$ /C	$Q_{\text{TH}}$ /C	$R_F$ /%
0.35	Pt	2.3	2.2	96.5
	Pt–Sn	17.9	17.9	99.3
	Pt–Re	18.8	18.6	99.1
0.45	Pt	14.1	13.9	99.2
	Pt–Sn	28.14	25.9	92.2
	Pt–Re	65.8	65.5	99.5
0.55	Pt	40	38.7	96.7
	Pt–Sn	50.1	40.1	97.9
	Pt–Re	65.1	64.8	99.6
0.65	Pt	69.1	68.6	99.3
	Pt–Sn	87.0	86.9	99.9
	Pt–Re	97.1	96.1	99.0

electricity recorded on a coulometer during the electrolyses was always close to 99%, thus corroborating the HPLC analyses.

In fact, AAL, AA and only traces of CO<sub>2</sub> were the oxidative derivatives of ethanol. AA was not detected on pure platinum at the lowest potential ( $0.4 \text{ V}$  vs RHE) as was stated by Hitmi et al. [35]. In fact, the authors have demonstrated that the reaction paths leading to AA are observed only at the end of the ‘double layer region’. At low potentials, Pt is not able to activate the oxygenated species coming from the solvent necessary to bring the extramolecular oxygen atom needed to oxidize the alcohol into the corresponding acid.

The amount of CO<sub>2</sub> detected with all the platinum based electrodes was higher at low potentials although the electrocatalytic activity represented by the quantities of electricity was the lowest. In fact, chemical adsorption of ethanol in the ‘hydrogen region’ generates strongly adsorbed species, from the breaking of the C–C bond, like CO which is oxidized to CO<sub>2</sub> at higher potentials. As expected, Pt is able to break the C–C bond of ethanol but it is unable to oxidize the corresponding adsorbates at low potentials leading to the same problems as for methanol. The addition of other metals such as Sn increases the electrode activity because they are able to activate the oxygen species from the solvent (H<sub>2</sub>O) at relatively low potentials. At  $0.4 \text{ V}$  vs RHE the quantity of electricity involved during 6 h of electrolysis is nearly ten times higher on PtSn or PtRe than on pure Pt although this positive effect did not affect the quantity of CO<sub>2</sub> produced, which remained small.

It is of interest to analyse the variation of the AA/AAL ratio. In fact, it was found that the AA/AAL ratio was independent of the catalyst loading so that all the problems related to the inaccuracy from the electrode preparation was not considered. As shown in Figure 5 the amount of AA was always lower than that of AAL in agreement with the consecutive reaction model. On

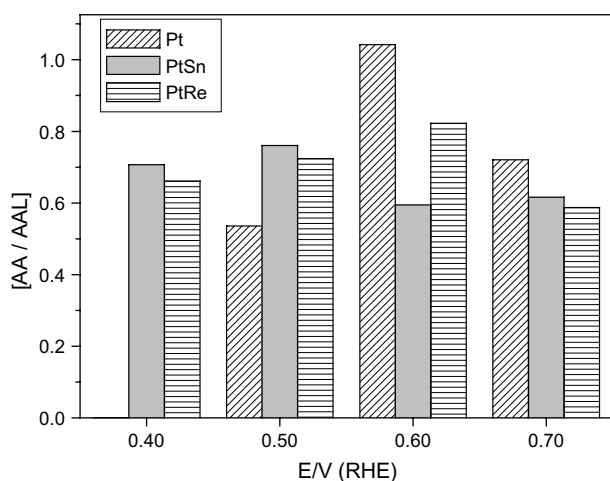
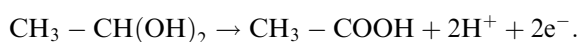
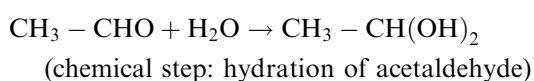


Fig. 5. AA/AAL ratio after 6 h of electrolysis at  $T = 293$  K of 0.1 M EtOH in 0.1 M  $\text{HClO}_4$  at different potentials from 0.35 to 0.65 V vs RHE obtained at Pt/C, PtSn (100:20)/C and PtRe (100:20)/C catalysts (30% metal loading).

both bimetallic catalysts the AA/AAL ratio is almost equivalent indicating that the reaction mechanism and the selectivity are not changed. Only the anode activity is promoted as shown in Table 2 and Figures 6(a) and (b).

The onset of the ethanol oxidation wave on PtSn catalysts is almost 175 mV more negative than that on Pt or PtRe electrodes (Figures 3 and 4), indicating that PtSn catalysts are less poisoned by the CO species. According to quantum-chemical calculations of the interactions of CO and OH with bimetallic surfaces [36], PtSn should be a good electrocatalyst for the oxidation of CO to  $\text{CO}_2$ . In fact, Morimoto et al. have shown that PtSn is active towards CO oxidation at potentials 100 mV lower than PtRu catalyst [37–39]. The authors have also confirmed these observations towards the oxidation of reformat gas [38]. Assuming that CO species adsorb only at platinum, the activation of oxygenated species at low potentials, as well as the modification of the platinum electronic structure, can be invoked as the result of the promoting effect of tin.

Otherwise, the reaction pathway involving four electrons to oxidize ethanol to acetic acid does not necessarily need the oxygenated species to be activated. If acetic acid is a secondary product of the oxidation of acetaldehyde, then the following mechanism including a chemical step can be considered:



The positive effect of Sn and Re seems to be related to the reactivity of the species resulting from the dissociative adsorption steps. The electrolysis results, and par-

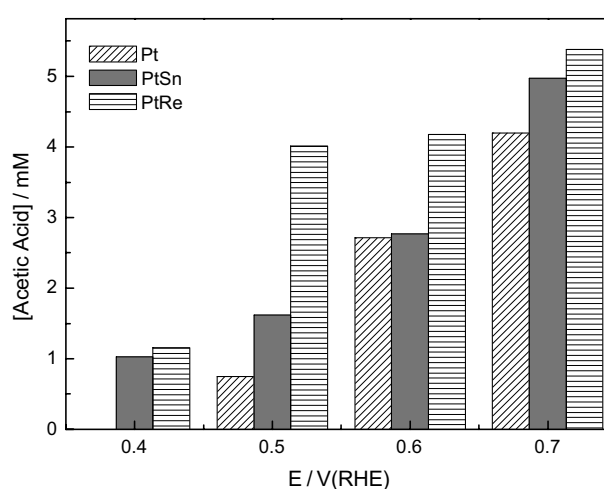
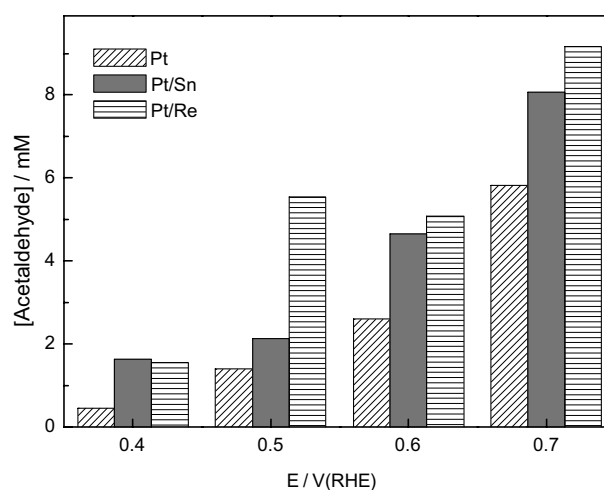


Fig. 6. AA and AAL amounts detected by HPLC after 6 h of electrolysis at  $T = 293$  K of 0.1 M EtOH in 0.1 M  $\text{HClO}_4$  at different potentials from 0.35 to 0.65 V vs RHE obtained at Pt/C, PtSn (100:20)/C and PtRe (100:20)/C catalysts (30% metal loading).

ticularly the AA/AAL ratio calculated at potentials higher than 0.4 V vs RHE, indicate that the oxidation of ethanol to acetaldehyde, on one hand, and the oxidation of the hydrated acetaldehyde to acetic acid, on the other hand, involve the well-known dehydrogenation processes during which the interactions between the reactants and the electrocatalytic sites – exclusively Pt under our experimental conditions – involve the C–H and the O–H bonds.

#### 3.4. Fuel cell tests

The electrode-membrane assemblies were prepared using a Nafion<sup>®</sup>117 membrane. Figure 7 represents the quantity of ethanol crossing the membrane separating an 1 M ethanol solution compartment and a water containing compartment as a function of time. The cross-over rate was evaluated close to  $1.3 \times 10^{-7}$  mol  $\text{s}^{-1}$   $\text{cm}^{-2}$ , while in the case of methanol the rate was found slightly lower ( $1.0 \times 10^{-7}$  mol  $\text{s}^{-1}$   $\text{cm}^{-2}$ ).

The performance of Pt/C, PtSn/C and PtRe/C electrocatalysts were evaluated in a single direct ethanol fuel

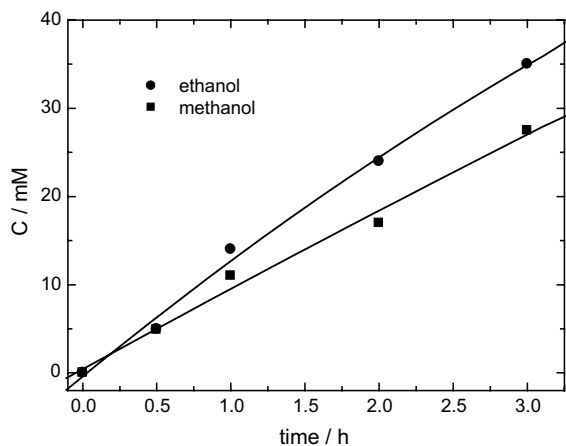


Fig. 7. Ethanol (●) and methanol (■) permeability measurements of a Nafion®117 membrane ( $T=293\text{ K}$ ).

cell at temperatures varying between 30 and 110 °C. The first remark concerns the positive effect of the temperature irrespective of the nature of the electrocatalysts. In

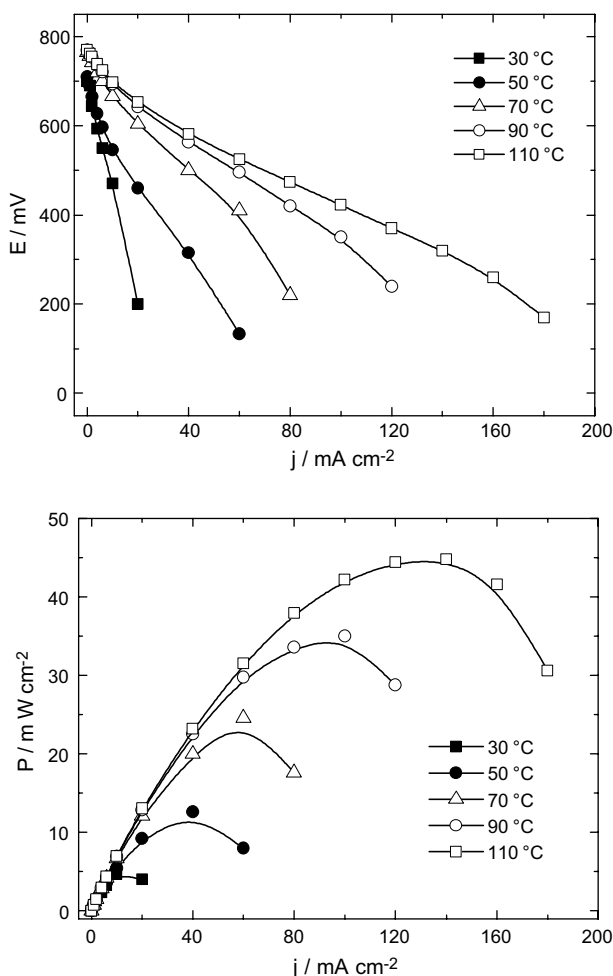


Fig. 8. Cell voltage  $E$  and power density  $P$  against current density  $j$  curves recorded in a single DEFC using a PtSn (100:20)/C anode (30% metal loading) of  $5\text{ cm}^2$  surface area, at different temperatures (cathode E-TEK, Nafion® 117 membrane,  $C_{\text{CH}_3\text{CH}_2\text{OH}} = 1.0\text{ M}$ ,  $P_{\text{CH}_3\text{CH}_2\text{OH}} = 1\text{ bar}$ ,  $P_{\text{O}_2} = 1.0\text{ bar}$ ). Effect of temperature.

the case of the PtSn/C anode, the maximum power density was 9 times higher at 110 °C than at 30 °C (Figure 8), reaching a maximum of  $45\text{ mW cm}^{-2}$ .

Pure platinum electrocatalyst from E-TEK was compared at 90 °C with the bimetallic Pt based electrocatalysts prepared in this work (Figure 9). The results are somewhat inconsistent with those obtained during long term electrolyses where PtRe electrocatalysts were found to be the most active towards ethanol oxidation particularly at potentials higher than 0.4 V vs RHE. However, the open circuit voltage (OCV) is 300 mV higher with a PtSn catalyst compared to PtRe and pure Pt which is consistent with the voltammetric measurements. At open circuit, it seems that the oxidation state of Re is not able to activate ethanol oxidation as was observed under controlled potential. PtSn catalyst leads to a maximum power density of  $35\text{ mW cm}^{-2}$  at 90 °C.

The OCV and the cell performances decrease due to ethanol cross-over. In fact, ethanol cross-over has a negative effect on the cathode performance because platinum is active towards ethanol oxidation. Moreover, the oxidation overvoltage  $|\eta_a(j)|$  may be decomposed

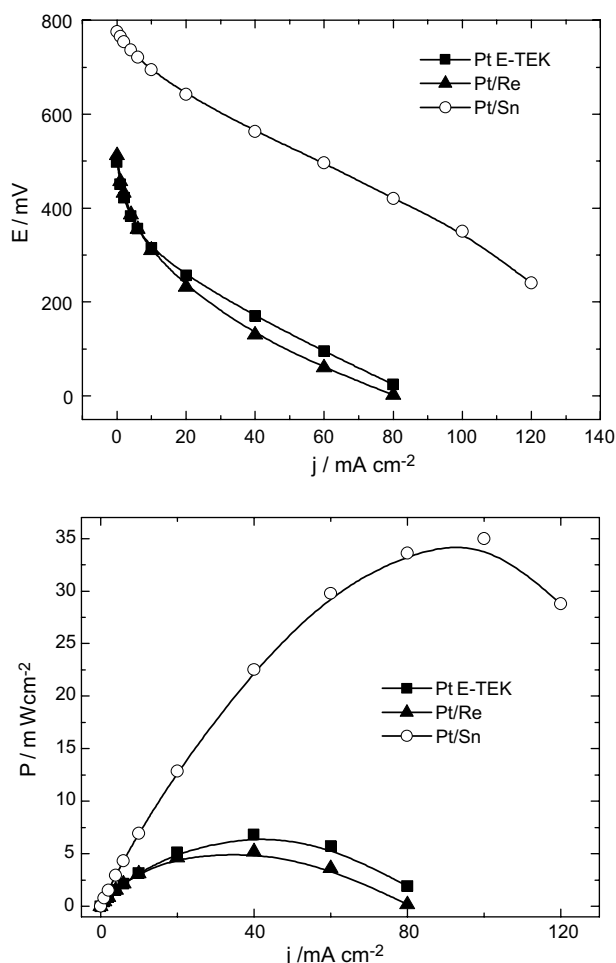


Fig. 9. Cell voltage  $E$  and power density  $P$  against current density  $j$  curves recorded in a single DEFC using Pt/C, PtSn (100:20)/C, PtRe (100:20)/C anodes (30% metal loading) of  $5\text{ cm}^2$  surface area at 90 °C (cathode E-TEK, Nafion® 117 membrane,  $C_{\text{CH}_3\text{CH}_2\text{OH}} = 1.0\text{ M}$ ,  $P_{\text{CH}_3\text{CH}_2\text{OH}} = 1\text{ bar}$ ,  $P_{\text{O}_2} = 1.0\text{ bar}$ ).

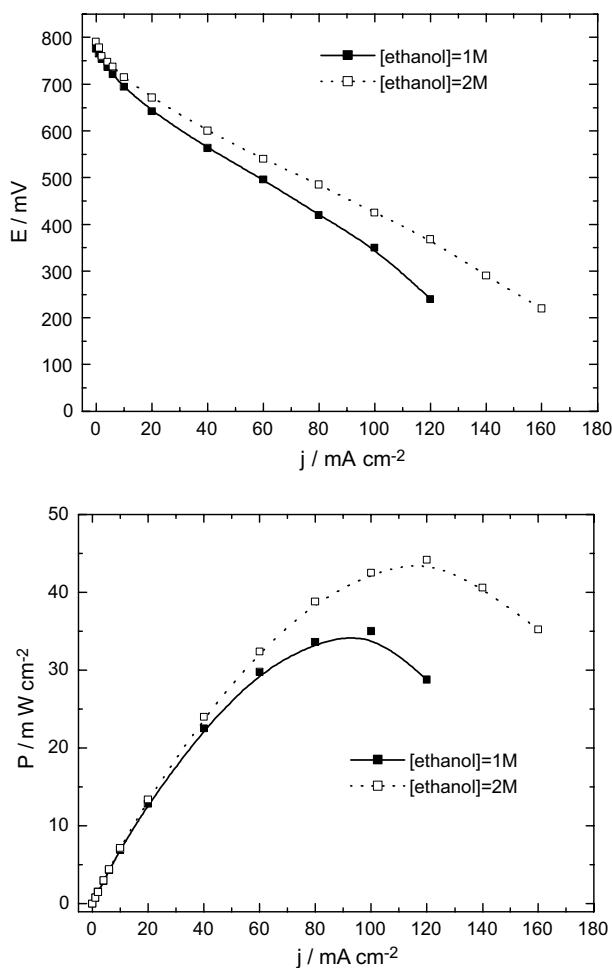


Fig. 10. Cell voltage  $E$  and power density  $P$  against current density  $j$  curves recorded in a single DEFC using a PtSn (100:20)/C anode (30% metal loading) of 5 cm<sup>2</sup> surface area at 90 °C for 1.0 and 2.0 M ethanol (cathode E-TEK, Nafion<sup>®</sup> 117 membrane,  $P_{\text{CH}_3\text{CH}_2\text{OH}} = 1$  bar,  $P_{\text{O}_2} = 1.0$  bar).

into the activation overvoltage and the concentration overvoltage:

$$|\eta_a(j)| = |\eta_a^{\text{act}}(j)| + |\eta_a^{\text{conc}}(j)| \quad (4)$$

so that the cross-over of ethanol through the membrane decreases its concentration in the anodic compartment and leads to an increase in the anodic overvoltage. Thus, cross-over has an effect, not only on the cathodic catalyst efficiency, but also on the anodic catalyst performance.

As for the DMFC [40, 41], the development of membranes less permeable to ethanol or cathodic catalysts more tolerant to ethanol should allow an increase in performance. On the other hand, increasing the ethanol concentration up to 2 M increases the performance of the fuel cell (Figure 10). The maximum power density rose up to 45 mW cm<sup>-2</sup> at 90 °C corresponding to an enhancement factor of 20% in the performance obtained with 1 M ethanol.

#### 4. Conclusion

The results obtained clearly show the positive effect of tin towards ethanol oxidation on Pt based electrocatalysts. However, rhenium which was expected from heterogeneous catalysis results to increase the electroactivity of platinum under DEFC conditions led to disappointing performances.

We have also shown that the atomic composition of the bimetallic catalysts has a significant effect on the electroactivity, as observed for PtRu catalysts used in a DMFC. In the latter case, the results published were somewhat inconsistent : some authors have shown that the optimal atomic ratio was close to 80:20 [42–44] whereas a 50:50 atomic ratio was suggested by other authors [45, 46]. The co-impregnation–reduction method to prepare the bimetallic catalysts allows easy control of the Pt/X atomic ratio and an atomic ratio Pt:X (X = Re, Sn) close to 100:20 appeared to be optimal for ethanol electrooxidation. However, the maximum metallic catalyst loading is limited to 30 wt %, which is relatively low for such applications.

The results obtained at 90 °C and 2 M ethanol in a DEFC are very promising, since the power density was close to 50 mW cm<sup>-2</sup> at a cell voltage close to 0.4 V.

#### Acknowledgements

We thank the ‘Conseil Général de la Région Poitou-Charente’ for financial support for this project.

#### References

1. J.M. Ogden, *Int. J. Hydrogen Energy* **24** (1999) 709.
2. J.M. Ogden, M.M. Steinbugler and T.G. Kreutz, *J. Power Sources* **79** (1999) 143.
3. H. Dohle, H. Schmitz, T. Bewer, J. Mergel and D. Stolten, *J. Power Sources* **106** (2002) 313.
4. V.P. Mc Connell, *Reinforced Plastics* **46** (2002) 8.
5. R. Nolte, *J. Power Sources* **4573** (2001) 1.
6. W. Wiese, B. Emonts and R. Peters, *J. Power Sources* **84** (1999) 187.
7. J.P. Breen, R. Burh and H.M. Coleman, *Appl. Catal. B: Environmental* **39** (2002) 65.
8. V. Klouz, V. Fierro, P. Denton, H. Katz, J.P. Lisse, S. Bouvot-Mauduit and C. Mirodatos, *J. Power Sources* **105** (2002) 26.
9. C. Yang, S. Srinivasan, A.S. Arico, P. Creti, V. Baglio and V. Antonucci, *Electrochem. Solid-State Lett.* **4** (2001) A31.
10. D. Chu, R. Jiang and C. Walker, *J. Appl. Electrochem.* **30** (2000) 365.
11. X. Ren, M.S. Wilson and S. Gottesfeld, *J. Electrochem. Soc.* **143** (1996) L12.
12. F. Delime, PhD thesis, University of Poitiers (1997).
13. A.S. Arico, P. Creti, P.L. Antonucci and V. Antonucci, *Electrochem. Solid-State Lett.* **1** (1998) 66.
14. Medis Technologies, *Fuel Cells Bull.* **2002** (2002) 5.
15. C. Lamy and J.-M. Léger, *J. Phys. IV* **4** (1994) C1.
16. P. Waszczuk, A. Wieckowski, P. Zelenay, S. Gottesfeld, C. Coutanceau, J.-M. Léger and C. Lamy, *J. Electroanal. Chem.* **511** (2001) 55.

17. T. Ioroi, N. Fujiwara, Z. Siroma, K. Yasuda and Y. Miyazaki, *Electrochem. Comm.* **4** (2002) 442.
18. L.F. Brown, *Int. J. Hydrogen Energy* **26** (2001) 381.
19. C. Song, *Catal. Today* **77** (2002) 17.
20. F. Joensen and J.R. Rostrup-Nielsen, *J. Power Sources* **105** (2002) 195.
21. C.L. Pieck, P. Marecot and J. Barbier, *Appl. Catal. A: General* **145** (1996) 323.
22. C. Roman-Martinez, D. Cazorla-Amoros, H. Yamashita, S. de Miguel and O.A. Scelza, *Langmuir* **16** (2000) 1123.
23. R.A. Rightmire, R.L. Rowland, D.L. Boos and D.L. Beals, *J. Electrochem. Soc.* **111** (1964) 242.
24. T. Iwasita and E. Pastor, *Electrochim. Acta* **39** (1994) 531.
25. T. Iwasita and E. Pastor, *Electrochim. Acta* **39** (1994) 547.
26. C. Lamy, A. Lima, V. Le Rhun, F. Delime, C. Coutanceau and J.-M. Léger, *J. Power Sources* **105** (2002) 283.
27. J. Wang, S. Wasmus and R.F. Savinell, *J. Electrochem. Soc.* **142** (1995) 4218.
28. J. Souza, F.J.B. Rabelo, I.R. de Moraes and F.C. Nart, *J. Electroanal. Chem.* **420** (1997) 17.
29. H. Hitmi, PhD thesis, University of Poitiers (1992).
30. F. Delime, J.-M. Léger and C. Lamy, *J. Appl. Electrochem.* **29** (1999) 1249.
31. C. Lamy, E.-M. Belgsir and J.-M. Léger, *J. Appl. Electrochem.* **31** (2001) 799.
32. A. Rezzouk, PhD thesis, University of Poitiers (1994).
33. M. Bonarowska, A. Malinowski and Z. Karpinski, *Appl. Catal. A: General* **188** (1999) 145.
34. A.K. Aboul-Gheit, M.F. Menoufy and A.K. El-Morsi, *Appl. Catal.* **61** (1990) 283.
35. H. Hitmi, E.-M. Belgsir, J.-M. Léger, C. Lamy and R.O. Lezna, *Electrochim. Acta* **39** (1994) 407.
36. T.E. Shubina and M.T.M. Koper, *Electrochim. Acta* **47** (2002) 3621.
37. Y. Morimoto and E.B. Yeager, *J. Electroanal. Chem.* **441** (1998) 77.
38. A.C. Boucher, PhD thesis, University of Poitiers (2002).
39. Y. Morimoto and E.B. Yeager, *J. Electroanal. Chem.* **444** (1998) 95.
40. T. Hatanaka, N. Hasegawa, A. Kamiya, M. Kawasumi, Y. Morimoto and K. Kawahara, *Fuel* **81** (2002) 2173.
41. N. Alonso-Vante, S. Cattarin and M. Musiani, *J. Electroanal. Chem.* **481** (2000) 200.
42. A. Kabbabi, R. Faure, R. Durand, B. Beden, F. Hahn, J.-M. Léger and C. Lamy, *J. Electroanal. Chem.* **444** (1998) 41.
43. H.A. Gasteiger, N. Markovic, P.N. Ross and E.J. Cairns, *J. Electrochem. Soc.* **141** (1994) 1795.
44. R. Ianello, V.M. Schmidt, U. Stimming, J. Stumper and A. Wallau, *Electrochim. Acta* **39** (1994) 1863.
45. H.N. Dinh, X. Ren, F.H. Garzon, P. Zelenay and S. Gottesfeld, *J. Electroanal. Chem.* **491** (2000) 222.
46. M. Watanabe, M. Uchida and S. Motoo, *J. Electroanal. Chem.* **229** (1987) 395.